

# Standardized Benchmark of Historical Compound Wind and Solar Energy Droughts Across the Continental United States

Cameron Bracken<sup>a,1</sup>, Nathalie Voisin<sup>a,2</sup>, Youngjun Son<sup>a,3</sup>, Sha  
Feng<sup>a,4</sup>, Osten Anderson<sup>a,5</sup>, Xiaodong Chen<sup>a,6</sup>, Li He<sup>a,7</sup>,  
Konstantinos Oikonomou<sup>a,8</sup>

<sup>a</sup> Pacific Northwest National Laboratory  
902 Battelle Boulevard, Richland, WA, 99352, USA.

This is a non-peer reviewed preprint submitted to EarthArXiv. The manuscript was submitted for publication in *Environmental Research: Energy*. Please contact the lead author with any comments or questions.

---

<sup>1</sup>cameron.bracken@pnnl.gov

<sup>2</sup>nathalie.voisin@pnnl.gov

<sup>3</sup>youngjun.son@pnnl.gov

<sup>4</sup>sfeng@pnnl.gov

<sup>5</sup>osten.anderson@pnnl.gov

<sup>6</sup>xiaodong.chen@pnnl.gov

<sup>7</sup>li.he@pnnl.gov

<sup>8</sup>konstantinos.oikonomou@pnnl.gov

1 Seasonal compound renewable energy droughts in the  
2 Unites States

3 Cameron Bracken<sup>a</sup>, Nathalie Voisin<sup>a,b</sup>, Youngjun Son<sup>a</sup>, Sha Feng<sup>a</sup>, Osten  
4 Anderson<sup>a</sup>, Xiaodong Chen<sup>a</sup>, He Li<sup>a</sup>, Konstantinos Oikonomou<sup>a</sup>

<sup>a</sup>*Pacific Northwest National Laboratory, Richland, WA, USA*

<sup>b</sup>*University of Washington, Seattle, WA, USA*

---

5 **Abstract**

Variable renewable energy (VRE) droughts are periods of low renewable electricity production due to natural variability in the weather and climate. These compound renewable energy droughts occur when two or more (typically wind and solar) generation sources are in low availability conditions at the same time. Compound wind and solar droughts are most commonly studied at the hourly and daily timescale due to the short-term nature of energy markets and battery storage capacity. However the seasonal time scale allows for the examination of broader climate and hydrologic patterns that influence a broader renewable energy portfolio and inform the needs for long-duration energy storage. In this study, we use a newly developed dataset of coincident renewable generation to characterize seasonal compound VRE droughts which include wind, solar and hydropower at grid-relevant spatial scales across the contiguous United States. Along with the frequency, duration, magnitude, and spatial scale, we specifically examine these climate patterns with a composite climate analysis. Results for the historical period (1982-2019) indicate that seasonal compound VRE droughts can last up to 5 months and occur most frequently in the Fall. While not an established “climate stress” to consider in reliability studies yet, we demonstrate the impact of seasonal energy droughts on a resource adequacy study over the Western US interconnection using a nodal bulk power grid model. We further discuss how seasonal compound VREs can inform the sizing of long-duration energy storage and market incentives to manage short-term extreme events like heat waves and cold snaps while considering seasonal conditions.

Corresponding Author: Cameron Bracken [cameron.bracken@pnnl.gov](mailto:cameron.bracken@pnnl.gov)

6 *Keywords:* energy droughts, renewable energy, long duration energy

## 8 **1. Introduction**

9 Variable renewable energy (VRE) droughts refer to naturally occurring  
10 periods of low energy availability from a resource such as wind, solar, and  
11 hydropower whose generation output is dependent on the weather or hydro-  
12 logic cycle. VRE droughts have been shown to have highly regional prop-  
13 erties that depend on both the local climatology and the specific makeup  
14 of the renewable generation and transmission infrastructure in a particular  
15 region [1, 2, 3, 4]. Compound VRE droughts refer to periods in which two  
16 or more generation sources are simultaneously experiencing drought condi-  
17 tions. Acute compound VRE events are necessarily more rare but can have  
18 much greater impacts to the grid in terms of increased costs, higher carbon  
19 emissions, or energy shortfalls [5, 6, 2].

20 Previous VRE drought studies [7, 2, 8, 3, 1, 9, 10, 11, 12, 13, 14, 15, 16, 17,  
21 18, 4, 19] typically focus on short timescales of hours to days which are partic-  
22 ularly relevant for grid stability [20] and energy storage [21]. Droughts which  
23 can occur on longer timescales of months to years are not commonly studied  
24 despite their implications for resource adequacy and at least higher green  
25 house gas emissions when renewable generation must be replaced [22, 23].  
26 In this study we seek to examine energy droughts on the seasonal timescale,  
27 which has typically been the focus of resource adequacy studies [24, 25].

28 Most studies of VRE drought do not consider hydropower due to the  
29 different timescale compared to wind and solar and the relative complexity  
30 of extending the analyses with large scale hydrologic modeling, water uses  
31 and associated water management. Raynaud et al. [1] analyze wind, solar  
32 and hydropower droughts independently in Europe but they do not consider  
33 compound events. Francois et al. [26] assess the statistical properties of solar  
34 and hydropower droughts to reduce their compound occurrences in Northern  
35 Italy. However, these studies incorporate hydrologic representations that are  
36 confined to run-of-river hydropower with no seasonal reservoir storage man-  
37 agement. Most et al. [27] examine compound wind, solar and hydropower  
38 droughts in Europe finding that appropriately managing reservoirs in winter  
39 is critical to mitigating and recovering from compound events. Woerman et  
40 al. [28] look at the complementarity of wind, solar and hydropower generation  
41 across Europe finding that droughts can be mitigated through a combina-  
42 tion of transmission and storage at the continental scale. We note that even

43 when water conditions might be low, hydropower operations are managed to  
44 provide a number of ancillary grid services such as operating reserves, volt-  
45 age support, blackstart and load factoring which are particularly valuable  
46 alongside wind and solar generation [29]. Hydropower, encompassing both  
47 run-of-river and reservoir storage types, is therefore important to consider in  
48 compound VRE drought studies that focus on longer timescales. Pumped  
49 storage hydro is economically designed to address shorter term storage needs  
50 and is not considered in this study.

51 Previous studies have shown that large-scale atmospheric circulations and  
52 climate modes, such as weather regimes and teleconnection patterns like the  
53 North Atlantic Oscillation (NAO) and Pacific-North American (PNA), have  
54 predictability for seasonal renewable energy generation [30, 31, 32, 33, 34,  
55 11, 35, 36, 14, 5, 15, 37]. For example, during the first quarter of 2015,  
56 the United States (U.S.) experienced a widespread and extended period of  
57 low surface wind speeds [38], which significantly impacted wind power gen-  
58 eration. Some wind farms failed to generate enough income to cover their  
59 steady payments, causing the value of certain assets to decrease. [33] found  
60 this wind energy drought event was due to high sea surface temperatures in  
61 the western tropical Pacific Ocean associated with a strongly positive phase  
62 of the North Pacific Mode, which played a crucial role in establishing and  
63 maintaining persistent low wind events. [39] demonstrated that the dom-  
64 inant source of skillful subseasonal-to-seasonal prediction for wind energy  
65 resources over the contiguous United States (CONUS) mainly comes from  
66 year-to-year variations of El Niño-Southern Oscillation (ENSO) in the trop-  
67 ical Pacific, which alters large-scale wind and storm track patterns over the  
68 CONUS. There are several studies examining relationships between climate  
69 conditions and the availability of specific renewable energy resources, such  
70 as solar or wind. However, research focusing on the atmospheric drivers of  
71 compound energy droughts is rare. [5] analyzed the relationship between  
72 compound solar radiation and wind speed droughts with weather systems  
73 and climate modes and found that these droughts occur most frequently in  
74 winter, affecting at least five key energy-producing regions in Australia on  
75 10% of days. The associated weather systems vary by season and drought  
76 type, but common features include widespread cloud cover and anticyclonic  
77 circulation patterns. Major climate modes are not strong predictors of grid-  
78 wide droughts, though regional variations exist that influence drought fre-  
79 quencies. In this study, we examine how large-scale circulations and climate  
80 modes contribute to seasonal compound VRE droughts over the CONUS.

81 The mechanisms identified may be useful for developing forecasting models  
82 or seasonal energy drought outlooks.

83 The impacts of VRE drought are not realized until they occur during pe-  
84 riods of high energy demand. One way to assess impacts to the energy system  
85 is to examine VRE droughts alongside energy demand which are known as  
86 VRE supply droughts or positive residual load (PRL) events [40, 4]. While  
87 this type of analysis can provide insights into potential regional energy short-  
88 falls, it lacks detailed system information such the impacts on energy prices,  
89 transmission congestion and unserved energy, and carbon emissions. Such  
90 information is provided by a nodal production cost model (PCM), a detailed  
91 unit commitment and economic dispatch model. In this paper we develop  
92 a CONUS-wide assessment of compound seasonal wind-solar-hydropower  
93 droughts which we complement with a case study that integrates five sepa-  
94 rate compound VRE drought events into the a PCM. The goal of this case  
95 study is to demonstrate the value of considering compound seasonal VRE  
96 drought in resource adequacy studies. Section 2 discusses the data used and  
97 how seasonal compound VRE drought events were identified, Section 3 ex-  
98 amines the historical properties, Section 4 looks at the spatial co-occurrence  
99 characteristics, Section 5 presents a composite climate analysis of the condi-  
100 tions that lead to compound VRE drought, Section 6 presents a case study  
101 that demonstrates how drought events can be incorporated into a power sys-  
102 tem model, and Section 7 is discussion.

## 103 **2. Identification of Seasonal Compound VRE Droughts**

104 Coincident and consistent plant-scale datasets for wind, solar [4], and hy-  
105 dropower [41] generation were analyzed to identify monthly energy drought  
106 events with 2020 infrastructure and historical weather conditions. Here, we  
107 briefly summarize the development of each dataset, as detailed descriptions  
108 are available in the cited literature. Historical meteorological data (1982-  
109 2019) from the Thermodynamic Global Warming (TGW) climate simulations  
110 [42] were utilized to estimate coincident energy generation from wind, solar,  
111 and hydropower renewable resources. In the TGW climate simulations, the  
112 Weather Research and Forecasting (WRF) model [43] was used to dynami-  
113 cally downscale the European Centre for Medium-Range Weather Forecast  
114 Version 5 Reanalysis (ERA5) [44].

115 Wind and solar generation was estimated for every utility scale wind  
116 and solar plant in the EIA 860 database [45]. Plant characteristics (turbine

117 height, rotor diameter, solar panel type, etc.) were combined with the TGW  
118 meteorology data using NREL’s reV model [46] to produce hourly plant-  
119 scale generation estimates. The solar radiation data was observed to have a  
120 high bias relative to observations in the National Solar Radiation Database  
121 (NSRDB)[47]. To account for this bias, the solar generation was bias cor-  
122 rected using NSRDB as a baseline. Some added detail is available in the  
123 supplemental material, for full details please see [48].

124 Hydropower generation was estimated at individual facilities based on  
125 integrated hydrologic modeling to simulate runoff, a river routing-reservoir  
126 operations-water management model for regulated streamflow, and a hy-  
127 dropower model. The calculations of surface and subsurface runoff were  
128 performed using the Variable Infiltration Capacity (VIC) model [49, 50],  
129 which was calibrated at each 1/16<sup>th</sup> degree grid cell using the daily runoff  
130 dataset from the Global Reach-level Flood Reanalysis (GRFR) ReachHy-  
131 dro product [51, 52]. The generated runoff was subsequently aggregated to  
132 1/8<sup>th</sup> degree grids and routed using the mosartwmpy model [53], a Python  
133 translation of the Model for Scale Adaptive River Transport with Water  
134 Management (MOSART-WM) [54, 55]. The mosartwmpy model simulates  
135 regulated streamflow influenced by water management components, includ-  
136 ing reservoir operations and water withdrawals. The data-driven approach  
137 [56] was implemented for reservoir operations with reasonable data coverage.  
138 Hydropower estimates are developed using the Blhydro model [41] which  
139 uses reservoir outflow, inflow, storage, and previous lagged power to esti-  
140 mate monthly power generation.

141 Seasonal compound VRE droughts are identified by first spatially aggre-  
142 gating all individual plants to the the Balancing Authority (BA) scale. BAs  
143 are entities in the U.S. where supply and demand must be balanced at all  
144 times and specifically need to use local resources to balance the local ”must-  
145 take” wind and solar resources. The BA represents a grid-relevant scale at  
146 which to analyze VRE droughts. BA-scale wind, solar, and hydropower gen-  
147 eration data are then temporally aggregated to the monthly timescale. The  
148 monthly timescale is used because it can represent droughts which last at  
149 least 1 month so they can represent seasonal drought events. Table 1 shows  
150 the considered BAs. In this study, a seasonal compound VRE drought is de-  
151 fined as any period of consecutive months for which the total generation from  
152 wind, solar and hydropower is below the 40th percentile for each generation  
153 type. For a single month a compound energy drought is identified if

$$q(W_t) < 0.4 \text{ and } q(S_t) < 0.4 \text{ and } q(H_t) < 0.4 \quad (1)$$

154 where  $q$  is the empirical quantile function using a Weibull plotting position,  
 155 and  $W_t$ ,  $S_t$ , and  $H_t$  are the total wind, solar, and hydro generation at time  
 156  $t$ , respectively. This means that each generation type individually must fall  
 157 below the 40th percentile, not the combined generation of all three sources.  
 158 This threshold was chosen to be representative of consistently low renewable  
 159 generation that still represents a range of drought events across the contiguous  
 160 U.S. Based on the threshold, the severity of compound VRE droughts is  
 161 defined as the normalized energy deficit below the threshold [4].

### 162 **3. Historical properties of seasonal compound VRE drought**

163 In this section we examine the historical frequency, duration, and sea-  
 164 sonality of compound VRE droughts in the CONUS. The seasonality and  
 165 seasonal complementarity of VRE generation can provide insights into when  
 166 and why compound droughts occur. For example a hypothetical region in  
 167 which wind, solar and hydropower are perfectly non-complementary, i.e. have  
 168 identical climatological patterns, would be highly susceptible to seasonal  
 169 compound drought. Conversely a perfectly complementary region would be  
 170 highly resilient against compound droughts if capacity are equivalent. Fig-  
 171 ure 1(a) shows the seasonal climatology of simulated generation from wind,  
 172 solar, and hydro in each of the BAs in this study. The solid lines represent  
 173 the median generation expressed as a capacity factor (generation divided by  
 174 capacity) and the transparent ribbons span the 5th to 95th percentile of  
 175 monthly generation. While wind and hydro have highly regionally-variable  
 176 seasonal climatologies, solar presents a similar pattern in almost every BA,  
 177 peaking in the early summer and falling off in the winter. At the monthly  
 178 scale, solar also has remarkably low inter-annual variability. Figure 1(b)  
 179 shows the number of seasonal VRE droughts across all BAs and all years,  
 180 using a 40th percentile threshold for each resource, where the threshold is  
 181 based on the monthly values and is fixed across the entire year. Compound  
 182 droughts are rare in Summer mainly because of the low solar inter-annual  
 183 variability and strong seasonality, although in some regions seasonally low  
 184 wind and hydropower also contribute. The Fall is the season most prone to  
 185 droughts with both the longest duration droughts and highest frequency of  
 186 occurrence. The fall is when hydro is typically the lowest in both snowmelt

BA	BA name	NERC IC*	Cluster	Hydro cap.† (GW)	Solar cap. (GW)	Wind cap. (GW)	Total cap. (GW)
AECI	Associated Electric Cooperative Inc.	Eastern	Midwest	0.03	0.005	1.84	1.875
AVA	Avista	Western	Inner West	1.17	0.0384	0.211	1.4194
BPAT	Bonneville Power Administration	Western	PNW	21.7	0.175	6.6	28.475
CISO	Calif. Ind. System Operator	Western	CA	6.46	29.4	11.6	47.46
ERCO	Electric Reliability Council of Texas	Texas	Midwest	0.57	9.71	54.7	64.98
IPCO	Idaho Power Company	Western	Inner West	2.03	0.633	1.41	4.073
ISNE	Ind. System Operator of New England	Eastern	Northeast	1.71	3.03	2.86	7.6
LDWP	L.A. Dept. of Water and Power	Western	CA	0.308	1.98	0.677	2.965
MISO	Midcontinent Ind. System Operator	Eastern	Midwest	2.4	4.08	52.1	58.58
NEVP	Nevada Power Company	Western	Inner West	0.0134	3.19	0.3	3.5034
NWMT	NorthWestern Energy	Western	Intermountain West	0.681	0.028	0.902	1.611
NYIS	New York Ind. System Operator	Eastern	Northeast	4.62	1.32	3.98	9.92
PACE	PacifiCorp East	Western	Intermountain West	0.27	2.37	5.11	7.75
PACW	PacifiCorp West	Western	PNW	1.13	0.568	1.37	3.068
PGE	Portland General Electric	Western	PNW	0.675	0.22	0.899	1.794
PJM	PJM Interconnection	Eastern	Northeast	3.31	9.07	19.7	32.08
PSCO	Public Service Company of Colorado	Western	Intermountain	0.0389	1.04	8.38	9.4589
PSEI	Puget Sound Energy	Western	PNW	0.346	0.001	0.734	1.081
SPA	Southwestern Power Authority	Eastern	Midwest	1.51	0.024	0.598	2.132
SRP	Salt River Project	Western	Inner West	0.0897	0.518	0.126	0.7337
SWPP	Southwest Power Pool	Eastern	Midwest	3.08	0.783	47.9	51.763
TVA	Tennessee Valley Authority	Eastern	TVA	4.87	0.581	0.0036	5.454
WACM	WAPA** - Colorado-Missouri	Western	Intermountain West	0.707	0.381	1.46	2.548
WALC	WAPA** - Lower Colorado	Western	Inner West	3.8	0.264	0.7	4.764

Table 1: Balancing authorities and their grouping used in this study with hydro, wind, and solar generation capacity represented in this study in gigawatts (GW). The Cluster column indicates the resulting clusters derived from a hierarchical clustering analysis in Section 5.

\*North American Electric Reliability Corporation Interconnection region

\*\*Western Area Power Administration

†Capacity

187 and rain driven regions which is consistent with national assessments [57].  
188 Wind can be either climatologically low or high in the fall and winter de-  
189 pending on the region, which, when high, helps to mitigate drought in those  
190 seasons in some regions. In Figure 1(c), we can see the spatial pattern of  
191 drought frequency: seasonal compound VRE droughts occur the most often  
192 in the west with a decreasing frequency moving toward the east. This is  
193 primarily due to the lower hydro seasonality and complementarity between  
194 wind and solar in these regions.

195 Figure 2 shows the seasonal distribution of compound VRE droughts from  
196 1982 to 2019 for each BA. In each stacked bar representing the annual total  
197 occurrences, the unit bar height is equivalent to one month within a specific  
198 season. The distribution over 38 years indicates that the majority of com-  
199 pound VRE droughts occur in fall and winter seasons, which is consistent  
200 with the previous section and other’s findings [33, 37, 5, 39]. Furthermore,  
201 these drought events are predominantly concentrated in the Western Inter-  
202 connection (WI; BPAT to WACM, colored in purple), whereas relatively  
203 smaller events are identified in the Eastern Interconnection (EI; AECI to  
204 PJM, colored in brown). The WI BAs, including CISO, NEVP, and WALC,  
205 experience a significant number of compound drought months during both  
206 fall and winter seasons, potentially due to similar low generation patterns  
207 across wind, solar and hydro during these seasons, as shown in Figure 1(a).  
208 As a result, in these BAs, prolonged VRE droughts from fall to winter could  
209 pose a risk to electricity supply, particularly when combined with increased  
210 demand driven by winter weather events, such as cold snaps [58]. In contrast,  
211 compound VRE droughts are infrequent in the EI BAs, including MISO and  
212 TVA, where monthly generation patterns are complementary. A few short-  
213 term compound drought months in summer are identified specifically in two  
214 EI BAs (SWPP and SPA), which may be linked to intermittent low wind  
215 generation with little within-year variation in wind, solar, and hydro gener-  
216 ation (Figure 1(a)). Certain BAs (PGE, MISO, TVA, ISNE, NYIS, and PJM)  
217 experience compound VRE droughts only during fall. These BAs typically  
218 show strong wind or hydro power generation patterns during winter (Figure  
219 1(a)).

#### 220 4. Seasonal co-occurrence and severity

221 In an interconnected grid, simultaneous occurrences of compound VRE  
222 droughts across BAs may critically impact the bulk power system reliability

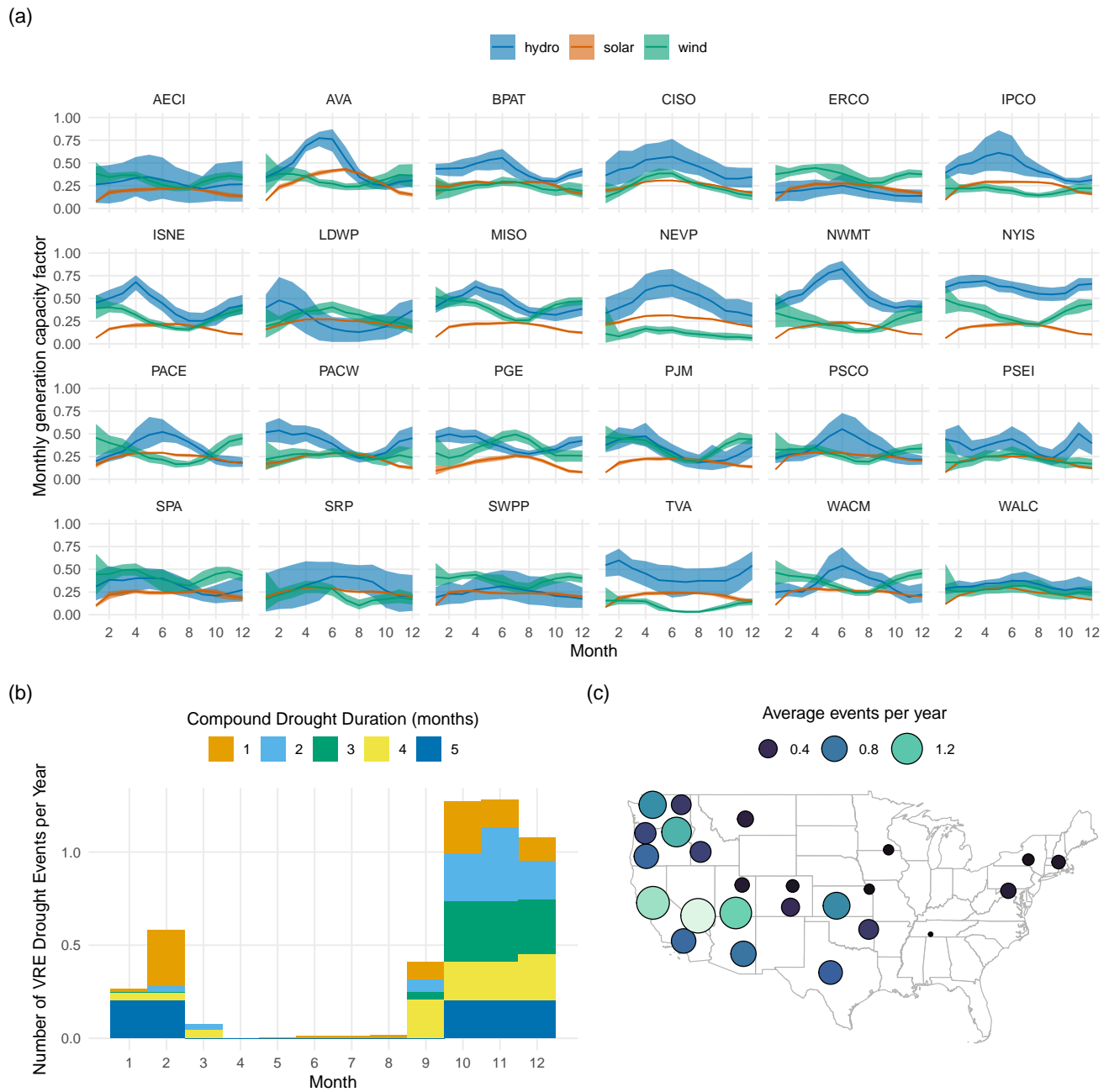


Figure 1: Historical properties of seasonal compound VRE drought: (a) shows the climatological patterns of wind, solar and hydro generation expressed as a capacity factor (generation divided by capacity) for each of the 18 BAs represented in this study. The solid lines represent the median monthly generation and the ribbons span from the 5th to 95th percentiles of the historical period (1982-2019). (b) Shows the seasonal occurrence of compound monthly VRE drought events where the bars are broken down by drought duration in months. (c) Shows the average compound VRE drought frequency for each BA.

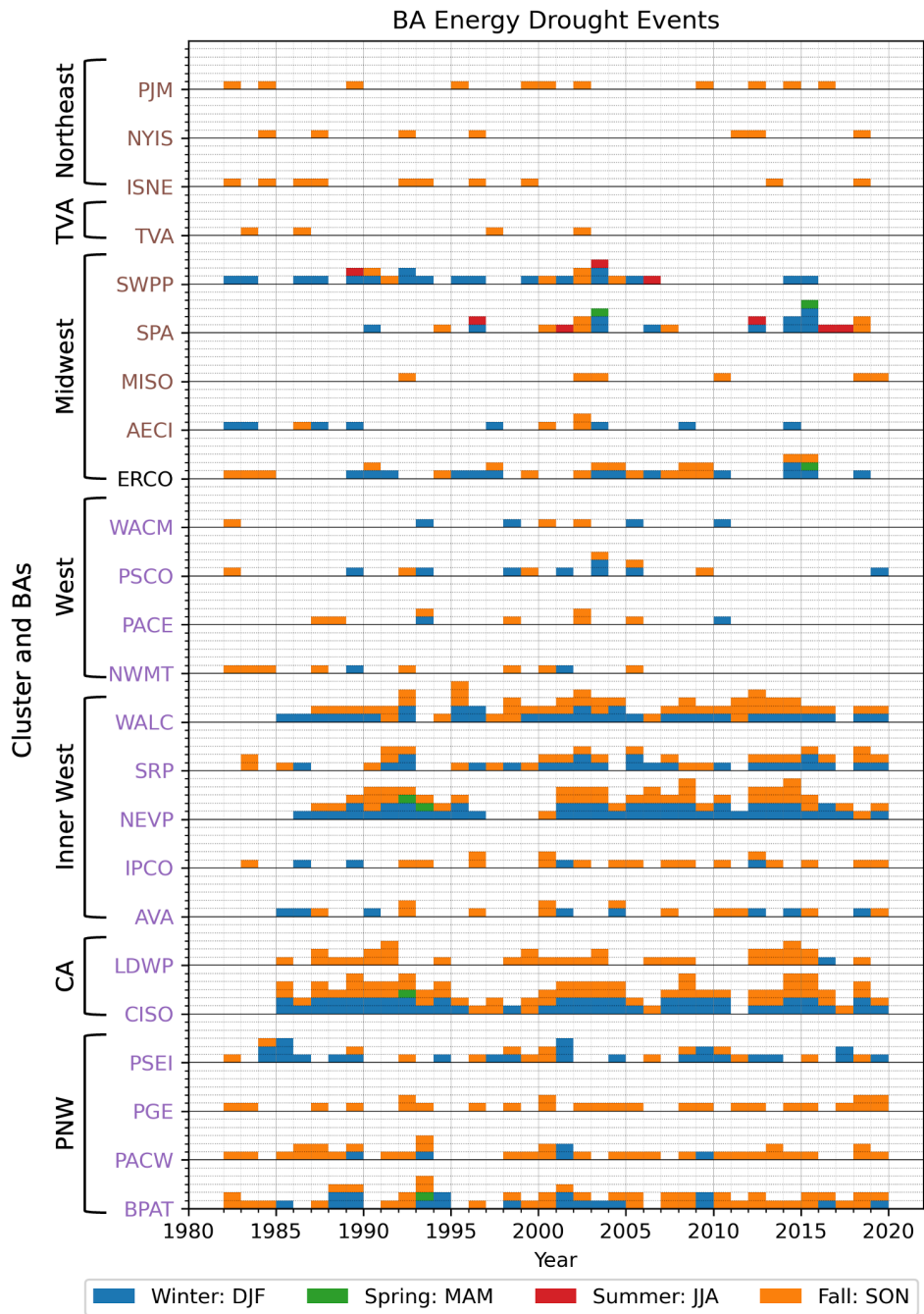


Figure 2: Number of compound energy drought months by season from 1982 to 2019. The unit height of each bar represents one month within a particular season. Note that the BAs in this figure are ordered to align with the clusters from West (bottom) to East (top), detailed in the following sections.

223 [59, 4] as adjacent regions are stressed with balancing their demand with  
224 their supply shortfall and may have limited regional coordination. Figure  
225 3(a) illustrates the co-occurrences of compound VRE droughts during the  
226 fall and winter seasons, with their frequencies represented by the thickness  
227 and color of connecting lines between pairs of BAs. Each BA is denoted as a  
228 circle, with its size proportional to the total number of VRE drought months,  
229 including both isolated and concurrent droughts. In fall, the co-occurrences  
230 of compound events are broadly distributed especially within WI BAs, and  
231 are temporally aligned with EI BAs despite their lower frequencies. In con-  
232 trast, during winter, the co-occurrences are particularly pronounced in the  
233 southwestern BAs such as CISO, NEVP, WALC, and SRP, with noticeable  
234 frequencies extending to limited portions of EI BAs, including AECI, SWPP,  
235 and SPA. The spatial distribution maps for fall and winter indicates two no-  
236 table trends: a decrease in frequency in the U.S. Pacific Northwest and an in-  
237 crease in frequency in the U.S. southwest and central regions. Consequently,  
238 the region vulnerable to coincident resource shortfalls shifts from the west-  
239 ern CONUS in fall to the southwestern and central CONUS in winter. These  
240 shifts are attributed to regional differences in the seasonality of wind, solar,  
241 and hydro generation, as shown in Figure 1(a). However, it is important  
242 to note that the concurrent occurrences (connecting lines in Figure 3(a)) do  
243 not account for the electricity transmission constraints, which need further  
244 consideration to understand their impacts on the interconnected grids. We  
245 also note that the Western and Eastern interconnections are not substan-  
246 tially connected however national transmission planning studies explore such  
247 opportunities [60], making this regional dependencies even more relevant for  
248 cost-benefit analyses.

249 In the supplementary material, Figure S1 quantifies concurrent VRE  
250 drought months between pairs of BAs over 38 years. The lower triangular  
251 elements count the co-occurring months of compound droughts during fall,  
252 whereas the upper triangular elements count them during winter. Similar to  
253 Figure 3(a), a high number of co-occurrences are identified within the WI  
254 BAs during fall. The most frequent co-occurrences in fall are between CISO-  
255 NEVP (35 months), followed by CISO-WALC (30 months) and CISO-BPAT  
256 (30 months). During winter, while the primary locations of co-occurrences  
257 remain similar, the CISO-BPAT connection weakens (15 months) and the  
258 NEVP-WALC connection strengthens (34 months). Overall, CISO emerges  
259 as a hotspot for compound VRE drought during both fall and winter.

260 As a measure of the combined severity of compound VRE droughts be-

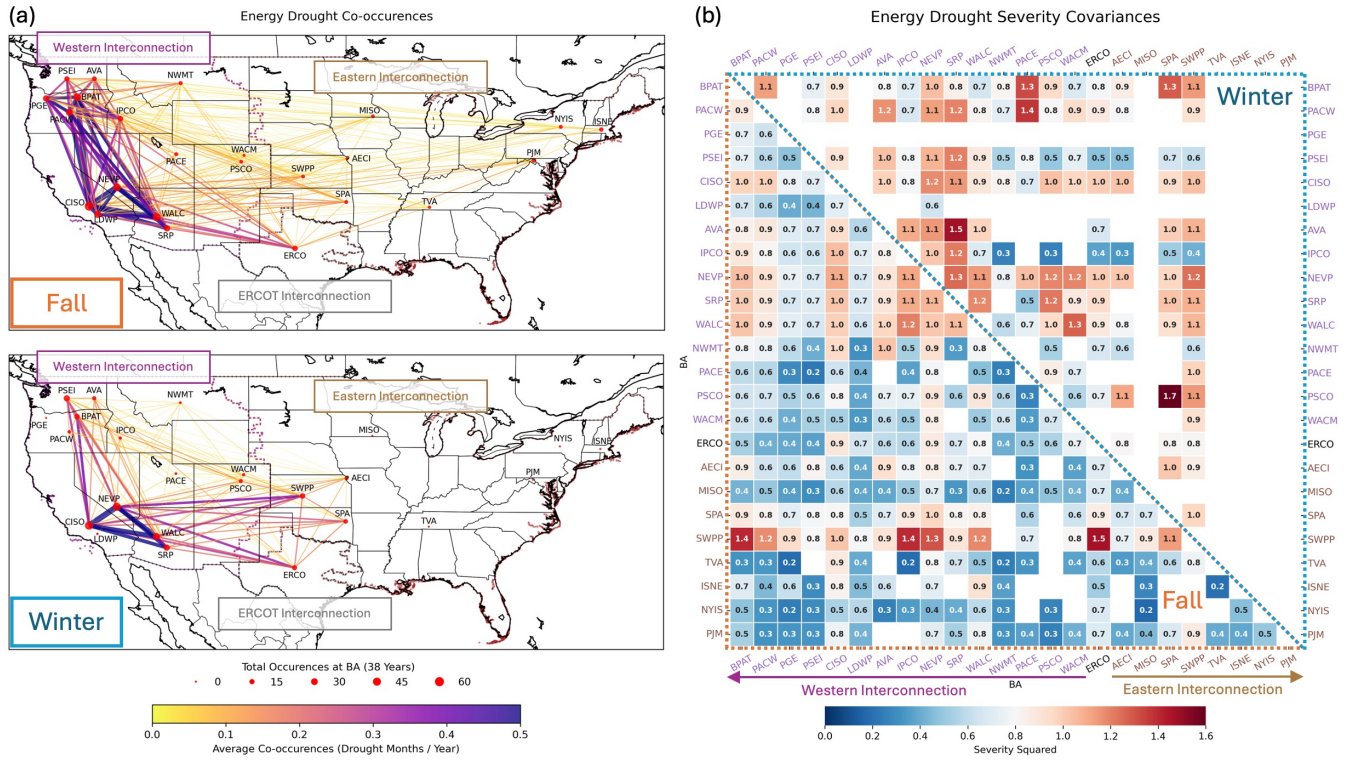


Figure 3: Seasonal patterns of compound VRE droughts: (a) co-occurrence patterns and (b) severity covariance heat map. In panel (a), the circle sizes represent the total number of VRE drought months at BAs, and the connecting line thicknesses indicate the average annual frequency of co-occurrences. The dashed lines delineate the boundaries of Interconnections. In panel (b), the severity covariances for fall and winter are shown in the lower and upper triangular sections, respectively. The BAs are sorted by NERC grid interconnection and Cluster in Table 2.

261 tween two BAs, we introduced the concept of severity covariance, which is  
 262 calculated based on Equation (2):

$$263 \quad \text{Severity Covariance } (i, j) = \frac{1}{N_D} \sum_{t=1}^{N_D} (z_{i,t} - \bar{z}_i)(z_{j,t} - \bar{z}_j) \quad (2)$$

264 where  $t$  represents drought months,  $z_i$  and  $z_j$  denote the standardized sever-  
 265 ity indices for a pair of BAs at locations  $i$  and  $j$ , respectively.  $N_D$  is the  
 266 total number of concurrent VRE drought months, and  $\bar{z}$  indicates the mean  
 267 of the standardized severity indices. Given that the combined severity of  
 268 VRE droughts is of our primary interest, only the severity indices during  
 269 drought months (i.e., negative values below the specified threshold) were  
 270 taken into consideration. In addition, the reference means were set to zero,  
 271 as the severity indices were derived from standardization to a normal distri-  
 272 bution. Therefore, the severity covariances quantify the co-occurring severity  
 273 trends of compound VRE droughts between pairs of BAs. Figure 3(b) shows  
 274 a heat map of the severity covariances across BAs. Compared to the co-  
 275 occurrences heat map in Figure S1, the severity covariances reveal different  
 276 patterns across BAs and between fall and winter seasons, indicating that the  
 277 frequency of occurrences is not necessarily correlated with their severity. In  
 278 winter, although compound VRE droughts are relatively infrequent across  
 279 the BAs (upper triangular elements of Figure S1), their severity tends to be  
 280 more intense. Notably, the severity covariance between SPA and PSCO is  
 281 identified as the highest (1.7 in Figure 3(b)) despite only two co-occurrences  
 282 over 38 years (two drought months in winter in Figure S1). Specifically, this  
 283 high severity covariance results from two severe compound events: one driven  
 284 by hydro droughts in both BAs and the other by low solar production in SPA  
 285 co-occurring with low hydro generation in PSCO. However, the impact of  
 286 these severe co-occurrences may be insignificant when considering electricity  
 287 transmission constraints, as these two BAs are located in different Intercon-  
 288 nections. During fall, most BAs tend to undergo relatively frequent (Figure  
 289 3(a) and lower triangular elements of Figure S1) but less severe compound  
 290 VRE droughts, with few exceptions. For example, the primary locations  
 291 of compound VRE droughts, such as CISO, NEVP, and WALC, show rela-  
 292 tively high severity covariance ( $> 1$ ), in addition to frequent co-occurrences  
 293 of compound VRE droughts.

## 294 5. Climate analysis

295 This section examines the climate mechanisms driving seasonal compound  
296 VRE droughts. Previous studies [37, 2, 11, 61, 16, 33, 32, 12, 14, 23] have  
297 demonstrated that seasonal energy droughts are closely related to large-scale  
298 atmospheric circulations and climate modes, which typically influence exten-  
299 sive geographic areas and are not confined to specific balancing authority  
300 definitions. Many BAs sharing similar geographic locations may be simul-  
301 taneously affected by the same weather or climate conditions. Therefore,  
302 before further investigating the atmospheric conditions inducing these com-  
303 pound VRE droughts, we conduct a hierarchical clustering analysis based on  
304 the correlations of the power generations among BAs. As a result, five clus-  
305 ters are generated (Figure 4): (1) PSEI, BPAT, PGE, and PACW; (2) AVA,  
306 IPCO, NEVP, WALC, and SRP; (3) CISO and LDWP; (4) TVA; (5) the  
307 remaining BAs (Figure S2). Given the geographical extent of the remaining  
308 BAs, we further divided them into three groups: the 5th cluster includes  
309 NWMT, PACE, WACM, and PSCO; the 6th cluster includes SWPP, SPA,  
310 AECI, ERCO, and MISO; the 7th cluster includes PJM, NYIS, and ISNE.

311 To find the large-scale conditions associated with droughts for given clus-  
312 tered BAs, we selected large-scale variables, including 500 hPa geopotential  
313 height, sea surface data, mean sea level pressure, relative humidity, temper-  
314 ature, and wind at the surface, 850 hPa, 500 hPa, and 200 hPa. We further  
315 composited the monthly anomaly of each variable by removing the climato-  
316 logical monthly mean between 1982 and 2019 for each from ERA5 monthly  
317 averaged reanalysis data [44, 62]. After clustering the BAs, we found that  
318 historically the number of seasonal droughts events range from 4 for the TVA  
319 cluster to a larger sample size for other clusters. To conduct a fair composite  
320 analysis (averaging the anomalies for each cluster), we limited each cluster to  
321 the top 4 events for the purposes of calculating the climatological anomalies.  
322 Therefore, for TVA, we averaged all the drought months in the composite  
323 analysis; for other clusters, we selected the four months with the most severe  
324 drought indices.

325 For this study, we also calculated the correlation between power gen-  
326 eration and the Arctic Oscillation (AO) [63, 64, 65], the North Atlantic  
327 Oscillation (NAO) [66], and the El Niño-Southern Oscillation Precipitation  
328 Index (ESPI) [67], obtained from the official National Oceanic and Atmo-  
329 spheric Administration (NOAA) website ([https://psl.noaa.gov/data/  
330 climateindices/list/](https://psl.noaa.gov/data/climateindices/list/)). Figure 5 shows the correlation coefficients between

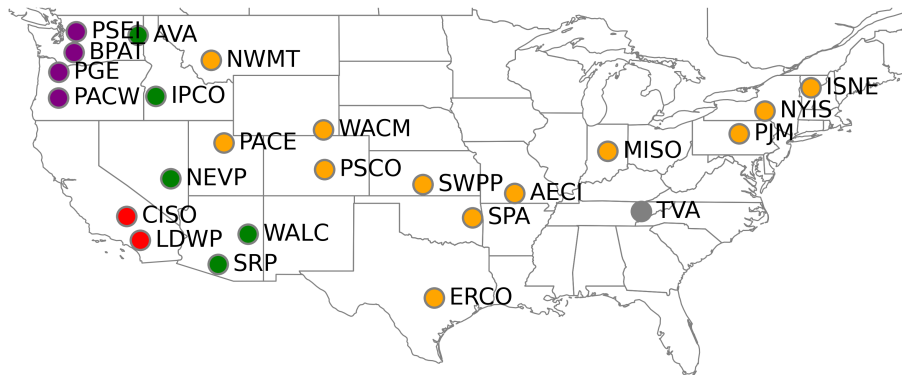
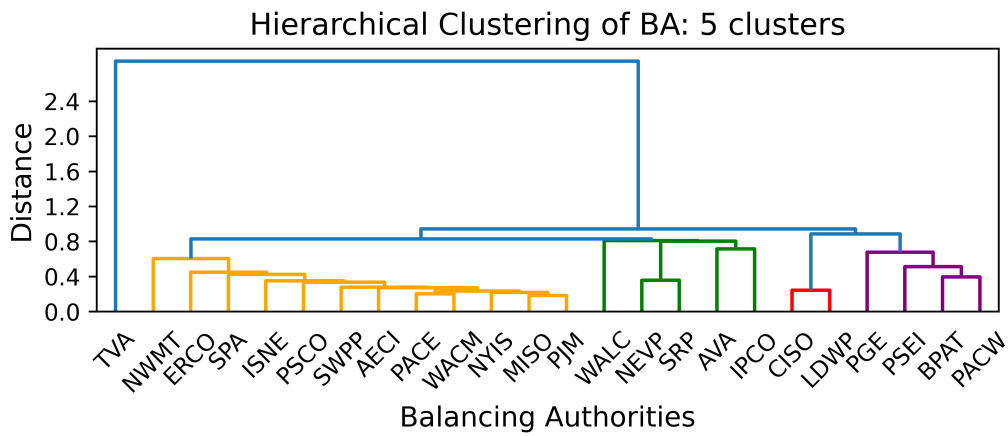


Figure 4: Clustered BAs and their geographic locations.

331 power generation and climate indices for each BA. While individual energy  
332 resources within these clusters may show correlations with climate indices,  
333 the aggregate power generation for these clusters does not always exhibit  
334 such relationships

335 For the PNW (PSEI, BPAT, PGE, and PACW) cluster, wind energy is  
336 the dominant renewable energy source, and it shows a strong correlation with  
337 the ESPI index. Additionally, the AO is correlated with power generation in  
338 two BAs within this cluster: BPAT and PACW. Due to the predominant role  
339 of wind energy, the correlation between wind energy and ESPI also drives the  
340 compound total power generation for this cluster. Furthermore, hydropower  
341 generation for PGE and PACW exhibits some correlations with the ESPI  
342 index.

343 In the CA (CISO and LDWP) cluster, there are minimal correlations  
344 between power generation and the three climate indices (AO, NAO, and  
345 ESPI). The only notable correlations are between hydropower generation for  
346 CISO with ESPI and NAO.

347 The Inner West (AVA, IPCO, NEVP, WALC, and SRP) cluster also shows  
348 rare coherent correlations. NAO is correlated with both solar and hydro  
349 generation for WALC, while ESPI is correlated with hydropower generation  
350 for NEVP and with wind energy for SRP.

351 The Intermountain West (NWMT, PACE, WACM, and PSCO) cluster  
352 is predominantly wind energy-focused, but there is little evidence showing  
353 strong correlations between solar or hydropower and climate indices. The  
354 correlation with wind energy influences the cluster's total energy generation.  
355 However, the only significant correlation observed within this cluster is be-  
356 tween NAO and wind generation for NWMT

357 The Midwest (SWPP, SPA, AECI, ERCO, and MISO) cluster exhibits  
358 different behaviors. While some significant correlations exist between single-  
359 source generation (e.g., solar and hydropower) and climate indices, these  
360 correlations are not evident in compound power generation. ESPI is corre-  
361 lated with solar generation for SWPP and with hydropower generation for  
362 other BAs in this cluster. NAO is highly correlated with solar overall, and  
363 AO shows correlation with hydropower generation for SWPP. However, there  
364 is no evident correlation between wind energy and the climate indices.

365 In the NE (PJM, NYIS, and ISNE) cluster, there is a high correlation be-  
366 tween NAO and solar generation across the entire cluster, as well as between  
367 NAO and hydropower generation for PJM. Similar to the fifth cluster, there  
368 is no evident correlation between wind generation and climate indices, and

369 the correlation rarely appears in the compound total energy.

370 The pattern in the TVA cluster is very similar to that in the NE cluster,  
371 with the exception that hydropower generation shows a correlation with  
372 ESPI.

373 Note that the Intermountain West, Midwest, and NE clusters are separated  
374 artificially; initially, they formed one larger cluster based on total power  
375 generation 4. This separation can be traced by no significant correlation with  
376 climate indices across these three clusters, except for the NAO in the case of  
377 NWMT.

378 The investigation into the weather mechanisms driving the occurrence  
379 of seasonal energy droughts across various regions highlights important atmospheric  
380 variables influencing energy resources. However, the direct application of these  
381 weather pattern descriptions for predictability remains challenging. For example,  
382 while we observe that an Arctic Ridge pattern can be associated with drought  
383 conditions in the Pacific Northwest (PNW: PSEI, BPAT, PGE, and PACW) cluster,  
384 it is not necessarily the case that every Arctic Ridge event results in a drought,  
385 nor is the duration of the Arctic Ridge always sufficient to establish a clear and  
386 robust causality.

387 To strengthen the focus on predictability, we have concentrated on regions  
388 where we have identified statistically significant connections between climate indices  
389 and renewable energy droughts. For instance, our analysis shows that in the California  
390 (CA: CISO and LDWP) cluster, specific climate indices such as the El Niño Southern  
391 Oscillation have a significant correlation with hydropower generation deficits. Detailed  
392 discussions and analyses of these regions with statistically significant connections are  
393 provided in the supplementary material.

394  
395 We acknowledge that the qualitative descriptions of weather patterns in other regions  
396 require further research to establish their predictive capability. Therefore, we have  
397 moved the detailed composite analyses of these regions to the supplementary material.  
398 This allows us to maintain a clear focus in the main text on regions where predictability  
399 based on climate indices is more established.  
400

## 401 **6. Case Study**

402 This section presents a case study of the potential impacts of these seasonal  
403 compound VRE droughts on grid operations in the western U.S. These impacts are  
404 studied on the WI using the WECC 2030 Anchor Data Set (ADS)

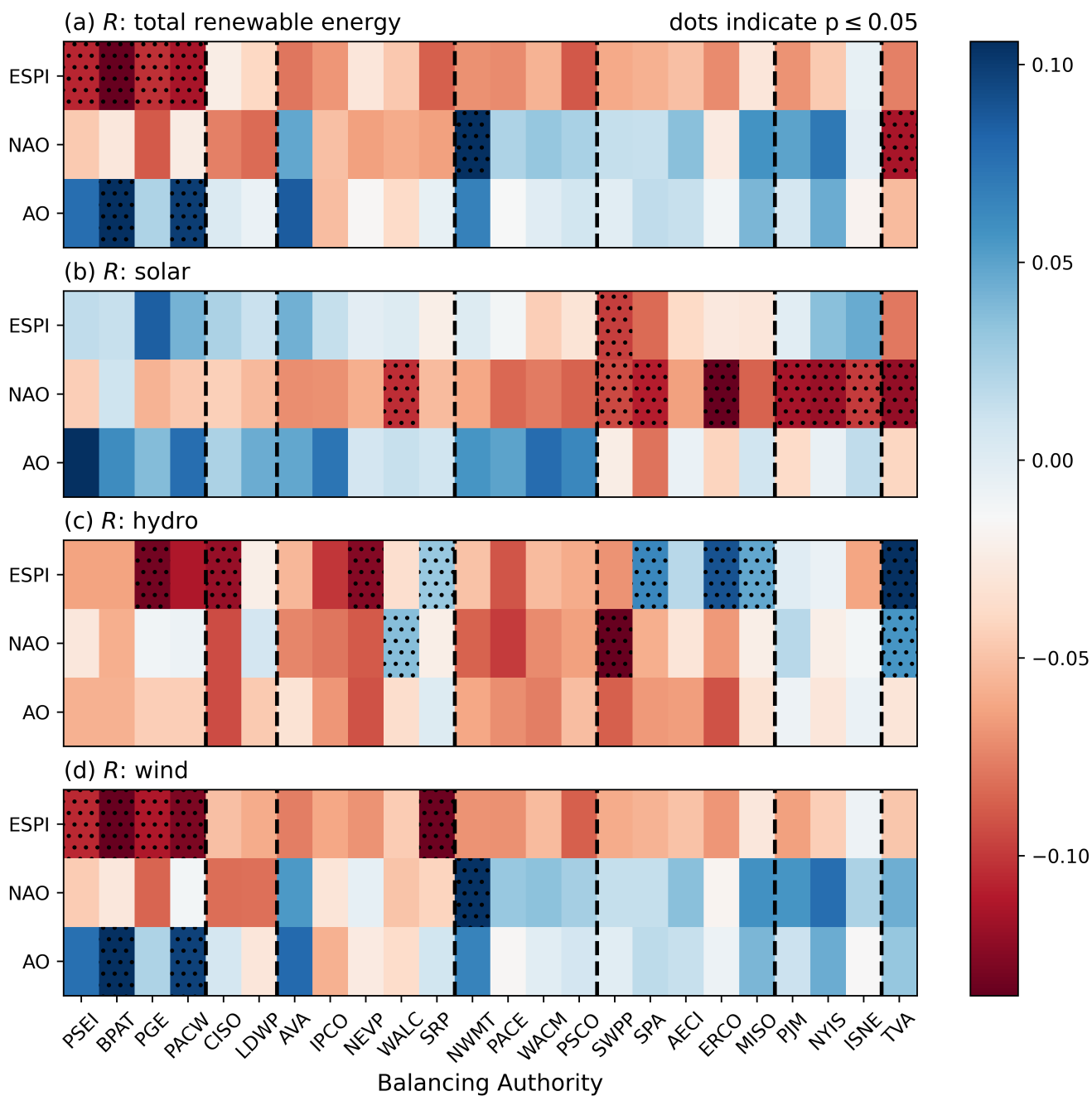


Figure 5: Heat map of the correlation ( $R$ ) between power generation and climate indexes for each BA. Note that the black dots indicate that the correlation is statistically significant when the  $p$ -value is less than the significance level of 0.05; the dashed lines between BAs indicate different clusters for BAs. (a) is for total power energy generation, (b) is for solar, (c) is for hydropower, and (d) is for wind generations.

405 Gridview test case. GridView, a grid operations model widely utilized in the  
406 industry, is used to model the behavior of dispatch. The WECC 2030 ADS  
407 is the base nodal dataset for the Western Interconnection baseline analysis  
408 [68]. The WECC 2030 ADS is a comprehensive scenario, incorporating input  
409 from all planning regions. It aims to project the Western Interconnection’s  
410 infrastructure for the year 2030, based on the best available knowledge at  
411 the time of the case’s release as well as existing state and federal laws. The  
412 transmission network topology for the WECC 2030 ADS Production Cost  
413 Model was carried over from a previous WECC study—the 2030HS (Heavy  
414 Summer) Power Flow dataset, which was compiled by the WECC Reliability  
415 Assessment Committee using GE PSLF software. The transmission topology  
416 was imported into the 2030 ADS Production Cost Model case as the basis  
417 for the transmission network topology and represents the best available pro-  
418 jection of anticipated new generation, generation retirements, transmission  
419 assets, and load growth in the 10-year planning horizon within the WECC  
420 grid planning community.

421 A full year in hourly resolution, at the nodal scale, is modeled for six  
422 scenarios. The first is presented as a control, and corresponds to a normal,  
423 non-drought year. The other scenarios correspond to drought events that  
424 were selected to represent the worst historical drought conditions across the  
425 entire WI. These are referred to as “Event 1” through “Event 5”, where  
426 Event 1 is the most extreme overall and Event 5 is the least extreme. Table  
427 2 shows the BA affected by each of the top 5 western US energy droughts  
428 along with the year and month the drought occurred. Five months from  
429 different years were identified that had the largest compound VRE drought  
430 severity across all BAs in the WI where the severity is defined as the total  
431 energy deficit below the 40th percentile drought threshold. Any BA drought  
432 that overlapped with the identified month was also captured in the input  
433 datasets for the GridView model. The droughts were used to modify the  
434 WECC 2030 ADS test case by proportionally lowering the VRE generation  
435 according to the historical generation during the identified droughts. For  
436 example if the wind in a BA had an average monthly capacity factor of 0.2  
437 during a drought month and the WECC 2030 ADS had an average monthly  
438 capacity factor of 0.4, then the hourly generation of all plants in the BA  
439 would be lowered by 50% to account for the drought conditions.

440 It is expected that drought years, as compared to typical years, will stress  
441 the grid in some way. In particular, reduced generation from solar, wind, and  
442 hydro, is expected to either reduce reliability, or increase dependence on gas

Table 2: The 5 worst (1 is the worst event) energy droughts affecting Western US BAs from 1982-2019. These 5 events are modeled in the case study.

Event	BA	Year	Month
1	AVA, BPAT, CISO, IPCO, NEVP, PACW, PSEI, SRP	2000	10, 11
2	AVA, BPAT, CISO, IPCO, NEVP, PACW, PGE, SRP, WALC	2019	10, 11
3	BPAT, CISO, NEVP, NWMT, PACW, PSCO, PSEI, SWPP, WALC	2001	10
4	AVA, CISO, IPCO, NEVP, PSEI, SRP, WALC	1985	10
5	CISO, NEVP, SWPP	1986	11, 12

443 resource. In practice, the WECC 2030 ADS features a robust generation  
 444 portfolio. For this analysis, no resource adequacy concerns, such as unserved  
 445 energy, are observed. Still, in less robust test cases, unserved energy may be  
 446 a concern.

447 Even without unserved energy, droughts still impose notable impacts on  
 448 grid operations. Figure 6 shows the increase in emissions and locational  
 449 marginal prices (LMPs) that exhibited during the drought as opposed to nor-  
 450 mal operation. For the sake of this analysis, the averages are computed and  
 451 compared across the extent of the drought in question with the normal, non-  
 452 drought year. This separates the impact of the drought from normal annual  
 453 variations in the behavior of these features. In general, drought events are  
 454 associated with a modest impact in the emissions. However, in some cases,  
 455 droughts result in spikes of the zonal emissions by well over 20% which is in  
 456 line with Voisin et al. [23] who showed that hydropower drought alone can  
 457 contribute to 10% increased emissions. This points towards the reduced gen-  
 458 eration due to drought being compensated for using gas-fired power plants.

459 Locational marginal prices (LMPs) convey the price of energy at a par-  
 460 ticular spatial location. In essence, they encode the availability of energy,  
 461 and are a function of several factors including fuel costs and transmission  
 462 congestion. Intuitively, droughts increase reliance on gas generation to serve  
 463 demand, thus leading to higher fuel component of LMPs. This behavior is  
 464 most heavily concentrated in the Northwest with LMPs increasing by 5-10%  
 465 in every event. Some regions actually have 5-10% lower LMPs during the  
 466 drought. This is due to reduced renewable and hydro generation resulting

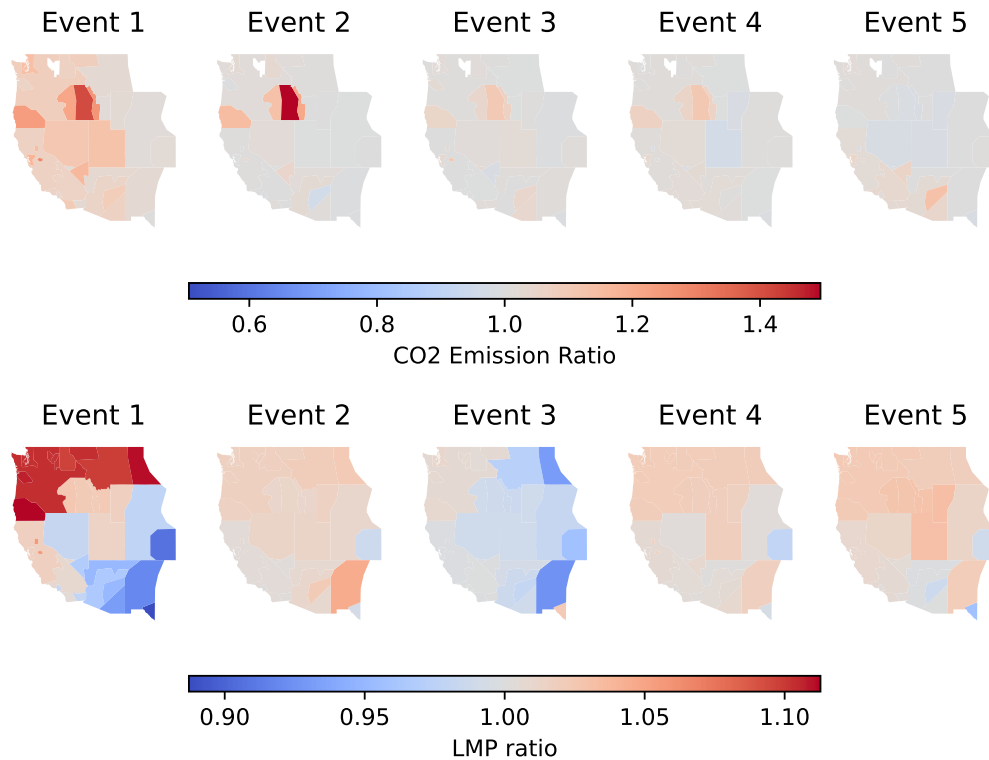


Figure 6: Average emission ratio (top row) and average locational marginal price (bottom row) ratio of each compound drought event divided by the baseline scenario (positive values indicate an increase in the energy drought scenario).

467 in less transmission congestion, and thus lower congestion component of the  
 468 LMP.

## 469 7. Discussion

470 The analysis of monthly timescale VRE droughts require long term cli-  
 471 mate simulations, representation of land surface processes and human sys-  
 472 tems dynamics. Seasonal compound VRE droughts in the contiguous U.S.  
 473 have diverse regional characteristics that stem from the complementarity of  
 474 the wind, solar and hydro generation. In the CISO BA (California), these  
 475 three renewable resources are almost perfectly non-complementary and con-  
 476 sequently we see that region with the highest frequency of compound VRE  
 477 drought. Conversely in the TVA BA (Tennessee), wind and hydro are al-

478 most perfectly complementary with solar and in that BA we see the lowest  
479 frequency of compound VRE drought. Furthermore, very few droughts occur  
480 in the summer in any BA which is driven by both the high solar and high  
481 hydro in the western U.S. Analogously, fall is the most prone to compound  
482 VRE droughts due to low hydro and tapering off solar. Wind tends not to be  
483 an overall driver of compound VRE drought due to how variable it is across  
484 regions. Based on these results we can conclude that climatological comple-  
485 mentarity is the main driver of the seasonal occurrence and frequency of VRE  
486 droughts at the monthly timescale. This insight indicates that climatology is  
487 a good indication to guide the development of renewable energy. While this  
488 is already performed in practice for individual resources, the insight further  
489 informs balancing regions in how to promote sustainable growth with a strate-  
490 gic distribution of capacities across the different resources. Some long term  
491 planning electricity models - also called capacity expansion models, often  
492 have a simplified representation of sub-annual dynamics with representative  
493 seasonal "stress periods" [69]. This study emphasizes the need to represent  
494 the complementarity between the renewable resources across all seasons and  
495 not select individual wind-solar-hydro supply curves which might lead to over  
496 building.

497 The spatial co-occurrences and co-severity of compound VRE droughts  
498 among BAs can provide valuable insights into the extent and intensity of their  
499 seasonal occurrences concentrated in specific regions. This aspect is critical  
500 to inform coordination across balancing regions with the exploration of new  
501 transmission path or re-sizing of the existing capacity. This co-occurrence can  
502 also inform the development of long term contracts across balancing regions.  
503 The primary regions of co-occurrences shift from the Western Interconnect  
504 BAs (CA, PNW, and Inner West clusters) in fall to the southwestern BAs  
505 (CA, Inner West, and Midwest clusters) in winter, due to the different sea-  
506 sonal responses of solar, wind, and hydro generation by region. Particularly,  
507 the BAs in California (CISO), Nevada (NEVP), and Arizona (WALC) ex-  
508 perience persistent co-occurrences of compound VRE droughts throughout  
509 both fall and winter. Based on these seasonal shifts around surrounding BAs,  
510 power system planning for compound VRE droughts could be optimized by  
511 considering spatial complementarity together with electricity transmission  
512 constraints and load seasonality also needs to be considered. Furthermore,  
513 the severity covariance matrix informs the historical patterns of the concur-  
514 rent intensity, which could be further integrated into power system planning  
515 to address deficiencies in electricity supply. The calculations of the sever-

516 ity covariances reveal that co-occurrences do not necessarily correlate with  
517 severity, as demonstrated by the BAs, which experience smaller but more  
518 intense events in winter. It is important to note that the correlation and  
519 covariance information provides only spatiotemporal alignment in the fre-  
520 quency and severity of compound VRE droughts, without accounting for the  
521 relative scales of electricity generation by energy source. This aspect may be  
522 important for the practical planning of power system grids.

523 The clustering analysis based on power generation correlations among  
524 BAs reveals a complex picture. Some BAs have one or two renewable energy  
525 sources which are strongly correlated to climate indices, while others have  
526 none. Although the total energy generation was utilized for clustering anal-  
527 ysis, the lack of correlation of specific resource may or may not propagate  
528 to influence the total energy generation, depending on the relative amount  
529 of each generation in each region. As a result, climate characteristics are  
530 unlikely to fully explain the occurrence of compound droughts; rather, they  
531 provide insight into the predictability of certain energy sources in specific re-  
532 gions. This phenomenon is particularly evident in regions such as the Pacific  
533 Northwest, which has abundant wind and hydropower resources, but limited  
534 solar power, and TVA, where solar and hydropower are plentiful but wind  
535 resources are minimal. Future studies should conduct detailed regional analy-  
536 ses to better understand the underlying mechanisms driving energy droughts  
537 and conclude on their predictability.

538 Studying single-resource energy droughts focuses on the impact of climate  
539 variability on individual renewable energy sources, allowing for clearer iden-  
540 tification of climate drivers and more straightforward mitigation strategies.  
541 For instance, analyzing wind energy droughts in isolation can directly link  
542 specific atmospheric circulation patterns, such as weather regimes (WRs),  
543 to wind speed anomalies. However, compound energy droughts involve the  
544 simultaneous deficit of multiple energy sources, adding complexity to the  
545 analysis. These compound events are influenced by a multitude of interact-  
546 ing climate variables and local factors, and our composite analysis reveals  
547 that specific weather patterns are indeed associated with energy compound  
548 droughts. This indicates that understanding these patterns can enhance  
549 forecasting and energy planning. Understanding the key differences between  
550 single and compound energy droughts is crucial for developing resilient en-  
551 ergy systems and improving forecasting methods that accurately account for  
552 the combined effects of different renewable energy sources.

553 The resource adequacy case study demonstrated that the planned 2030

554 infrastructure for the Western US would be robust to compound energy  
555 droughts with enough gas generation capacity held to meet demand in even  
556 the most extreme compound VRE droughts. The WECC 2030 ADS case  
557 dates back to 2020 when governmental policies were not targeting a substan-  
558 tial shift in energy generation portfolio and had a low end of wind and solar  
559 penetration with respect to other projections [70, 71, 60]. We anticipate that  
560 this library of compound wind-solar-hydro drought events will have a growing  
561 interest as the generation portfolio includes more of those resources. We also  
562 note that this library of events to guide resource adequacy studies needs to be  
563 complemented with the consideration for the load seasonality. For example,  
564 Yates et al. [72] demonstrated that the California irrigation load increase by  
565 6 percent in times of hydrological drought when hydropower resources are  
566 reduced by 20 percent. In addition, energy storage is recognized as a critical  
567 fleet component for shifting energy from hours with plentiful generation to  
568 hours with high load. In the case of seasonal droughts, long term duration  
569 energy storage with time scale of weeks and months may be necessary to  
570 maintain grid reliability and price volatility.

571 These results have implications for the long-term grid planning, especially  
572 in a decarbonized or low carbon future grid. Current storage technology and  
573 peaking capability may not be sufficient to mitigate droughts which last many  
574 months in duration. As renewable buildout continues the need for long du-  
575 ration energy storage will likely increase if we are to ensure future demands  
576 are met. To evaluate potential impacts, individual BAs should assess com-  
577 pound drought characteristics across multiple scales. For example, if low  
578 production periods within a seasonal drought occur relatively uniformly vs  
579 concentrated during smaller periods of the drought, could strongly influence  
580 the amount and type of energy storage required. Mitigating strategies for  
581 energy droughts such as investment in storage, transmission, or other gen-  
582 eration sources will be regionally specific and need to be tailored by each  
583 BA to meet their unique needs. Such strategies should be developed with a  
584 comprehensive understanding of local climate patterns, electricity generation  
585 and load profiles, and other factors that affect grid reliability.

## 586 **8. Limitations**

587 One limitation of this study is that load was not considered along side  
588 generation. Considering load is important for resource adequacy considera-  
589 tions at this time scale. For example, Fall was identified as the season with

590 the most likely compound VRE drought events, but this season typically has  
591 mild temperatures in the US so the grid impacts of such events are uncertain.  
592 Future studies may account for the dynamics between VRE drought  
593 events and load, such as high air conditioning loads and suppression of wind  
594 generation during heat domes. Evaluating events of compounded load and  
595 VRE drought may identify more stressful grid operation conditions.

596 Our results indicate some inconsistency between hydropower energy deficits  
597 and their climate proxies (IWV and VPD), particularly in regions like the  
598 TVA, Midwest, Intermountain, and Inner West. Hydropower is subject to  
599 human management, especially for dams where the occurrence of hydropower  
600 droughts is linked to atmospheric and hydrological drought conditions over  
601 extended periods of time. An accurate explanation of the connection between  
602 hydropower droughts and climate requires examining much longer timescales,  
603 often multiple years. Therefore, a minimum time span must be established to  
604 effectively use climate and weather patterns to explain hydropower droughts.  
605 Additionally, since the time scales of wind and solar are much shorter it would  
606 be beneficial to find an approach which allows for each resource to be included  
607 at the time scale with the most impact, such as a wind and solar drought  
608 during a heat wave which occurs during a period of hydrologic drought.

## 609 **9. Conclusion**

610 This study provides an analysis of compound wind, solar and hydropower  
611 seasonal energy droughts across the contiguous United States. Hydropower  
612 is by far the most complex component of the renewable droughts, requiring  
613 climate, land surface and water management modeling. Hydropower neces-  
614 sarily operates at a different timescale than wind or solar, necessitating a  
615 longer seasonal view of variable renewable droughts and strategies in man-  
616 aging multiple water uses. At this seasonal timescale, weather variability be-  
617 comes less important than the climatological complementarity of generation  
618 resources. Regions which have highly complementary resources for similar  
619 generating capacities will experience less compound drought and visa-versa.  
620 While this is an intuitive result, it is important to quantify to aid in regional  
621 planning and to prevent overbuilding. Additionally, our analysis identifies  
622 transmission-connected regions which have high risk for compound variable  
623 renewable energy droughts to co-occur, which can support transmission plan-  
624 ning adequacy and reliability studies.

625 Our climate analysis has indicated that predicting certain renewable sources  
626 at the seasonal scale may be possible in some regions of the contiguous United  
627 States. The atmospheric conditions which lead to compound droughts are  
628 complex and prediction of these compound events will require further study.

629 The case study presented serves as an example of how renewable energy  
630 drought data can be incorporated into production cost models to determine  
631 energy prices, transmission congestion, and carbon emissions during renew-  
632 able drought events. Our results indicated that the modeled 2030 infras-  
633 tructure was robust in the sense there was no unserved energy but this may  
634 change as wind and solar are rapidly developed. The compound droughts  
635 we identified using coincident data may serve as a new baseline for resource  
636 adequacy planning. While coincident wind-solar-load datasets are necessary  
637 for reliability studies and understand storage and reserve needs, this study  
638 indicates that hydropower drought conditions may be paired with other wind-  
639 solar-load datasets for the purpose of evaluating compound multi-scale ex-  
640 treme events, in some regions like the snowmelt dominated Western US. Such  
641 mix and match requires further evaluation and are scale-dependent and the  
642 provided analytics can support such regional evaluation.

## 643 10. Data Availability

644 The data used in this paper is available on Zenodo: [https://zenodo.](https://zenodo.org/records/14270835)  
645 [org/records/14270835](https://zenodo.org/records/14270835). The code used to reproduce the analysis and pro-  
646 duce figures is available on GitHub: <https://github.com/GODEEEP/seasonal-energy-droughts>.

## 647 11. Acknowledgments

648 This research was supported by the Grid Operations, Decarbonization,  
649 Environmental and Energy Equity Platform (GODEEEP) Investment, under  
650 the Laboratory Directed Research and Development (LDRD) Program at  
651 Pacific Northwest National Laboratory (PNNL). The study leverages the  
652 TGW climate datasets developed by U.S. DOE Office of Science multisector  
653 dynamics program as part of the IM3 and HyperFACETS projects. This work  
654 leverages the capabilities of mosartwmpy, a Python version of the MOSART-  
655 WM model supported by the U.S. Department of Energy, Office of Science, as  
656 part of research in MultiSector Dynamics, Earth, and Environmental Systems  
657 Modeling Program and enhanced by the Energy Efficiency and Renewable  
658 Energies - Hydrological Sciences Program. This work also leverages early

659 formulation developed under the HydroWIRES B1 project (grant 75563)  
660 sponsored by the Water Power Technologies Office under the HydroWIRES  
661 initiative. This research used resources of the Pacific Northwest Research  
662 Computing at the PNNL, which is a DOE Office of Science User Facility. The  
663 PNNL is a multi-program national laboratory operated by Battelle Memorial  
664 Institute for the U.S. Department of Energy (DOE) under Contract No.  
665 DE-AC05-76RL01830. Accordingly, the U.S. Government retains and the  
666 publisher, by accepting the article for publication, acknowledges that the U.S.  
667 Government retains a nonexclusive, paid-up, irrevocable, worldwide license  
668 to publish or reproduce the published form of this manuscript or allow others  
669 to do so, for U.S. Government purposes.

## 670 References

- 671 [1] D. Raynaud, B. Hingray, B. François, J. D. Creutin, Energy droughts  
672 from variable renewable energy sources in european climates, *Renew-*  
673 *able Energy* 125 (2018) 578–589. doi:[https://doi.org/10.1016/j.](https://doi.org/10.1016/j.renene.2018.02.130)  
674 [renene.2018.02.130](https://doi.org/10.1016/j.renene.2018.02.130).
- 675 [2] N. Otero, O. Martius, S. Allen, H. Bloomfield, B. Schaeffli, Character-  
676 izing renewable energy compound events across europe using a logistic  
677 regression-based approach, *Meteorological Applications* 29 (5) (2022)  
678 e2089. doi:<https://doi.org/10.1002/met.2089>.
- 679 [3] N. Otero, O. Martius, S. Allen, H. Bloomfield, B. Schaeffli, A copula-  
680 based assessment of renewable energy droughts across europe, *Renew-*  
681 *able Energy* 201 (2022) 667–677. doi:[https://doi.org/10.1016/j.](https://doi.org/10.1016/j.renene.2022.10.091)  
682 [renene.2022.10.091](https://doi.org/10.1016/j.renene.2022.10.091).
- 683 [4] C. Bracken, N. Voisin, C. D. Burleyson, A. M. Campbell, Z. J. Hou,  
684 D. Broman, Standardized benchmark of historical compound wind and  
685 solar energy droughts across the continental united states, *Renewable*  
686 *Energy* 220 (2024) 119550. doi:[https://doi.org/10.1016/j.renene.](https://doi.org/10.1016/j.renene.2023.119550)  
687 [2023.119550](https://doi.org/10.1016/j.renene.2023.119550).  
688 URL <http://dx.doi.org/10.1016/j.renene.2023.119550>
- 689 [5] D. Richardson, A. J. Pitman, N. N. Ridder, Climate influence on com-  
690 pound solar and wind droughts in australia, *npj Climate and Atmo-*  
691 *spheric Science* 6 (1) (Nov. 2023). doi:[https://doi.org/10.1038/](https://doi.org/10.1038/s41612-023-00507-y)  
692 [s41612-023-00507-y](https://doi.org/10.1038/s41612-023-00507-y).

- 693 [6] H. Lei, P. Liu, Q. Cheng, H. Xu, W. Liu, Y. Zheng, X. Chen, Y. Zhou,  
694 Frequency, duration, severity of energy drought and its propagation  
695 in hydro-wind-photovoltaic complementary systems, *Renewable Energy*  
696 230 (2024) 120845. doi:[https://doi.org/10.1016/j.renene.2024.](https://doi.org/10.1016/j.renene.2024.120845)  
697 120845.
- 698 [7] V. Gburčik, S. Mastilović, Željko Vučinić, Assessment of solar and wind  
699 energy resources in serbia, *Journal of Renewable and Sustainable Energy*  
700 5 (4) (2013) 041822. doi:<https://doi.org/10.1063/1.4819504>.
- 701 [8] P. E. Bett, H. E. Thornton, The climatological relationships between  
702 wind and solar energy supply in britain, *Renewable Energy* 87 (2016)  
703 96–110. doi:<https://doi.org/10.1016/j.renene.2015.10.006>.
- 704 [9] M. M. Miglietta, T. Huld, F. Monforti-Ferrario, Local complementarity  
705 of wind and solar energy resources over europe: An assessment study  
706 from a meteorological perspective, *Journal of Applied Meteorology and*  
707 *Climatology* 56 (1) (2017) 217–234. doi:[https://doi.org/10.1175/](https://doi.org/10.1175/jamc-d-16-0031.1)  
708 [jamc-d-16-0031.1](https://doi.org/10.1175/jamc-d-16-0031.1).
- 709 [10] B. François, B. Hingray, D. Raynaud, M. Borga, J. D. Creutin, Increasing  
710 climate-related-energy penetration by integrating run-of-the river  
711 hydropower to wind/solar mix, *Renewable Energy* 87 (2016) 686–696.  
712 doi:<https://doi.org/10.1016/j.renene.2015.10.064>.
- 713 [11] K. van der Wiel, H. C. Bloomfield, R. W. Lee, L. P. Stoop, R. Black-  
714 port, J. A. Screen, F. M. Selten, The influence of weather regimes on  
715 european renewable energy production and demand, *Environmental Re-*  
716 *search Letters* 14 (9) (2019) 094010. doi:[https://doi.org/10.1088/](https://doi.org/10.1088/1748-9326/ab38d3)  
717 [1748-9326/ab38d3](https://doi.org/10.1088/1748-9326/ab38d3).
- 718 [12] M. Gonzalez-Salazar, W. R. Pogonietz, Making use of the complemen-  
719 tarity of hydropower and variable renewable energy in latin america:  
720 A probabilistic analysis, *Energy Strategy Reviews* 44 (2022) 100972.  
721 doi:<https://doi.org/10.1016/j.esr.2022.100972>.
- 722 [13] J. A. Ferraz de Andrade Santos, P. de Jong, C. Alves da Costa,  
723 E. A. Torres, Combining wind and solar energy sources: Potential for  
724 hybrid power generation in brazil, *Utilities Policy* 67 (2020) 101084.  
725 doi:<https://doi.org/10.1016/j.jup.2020.101084>.

- 726 [14] H. C. Bloomfield, C. M. Wainwright, N. Mitchell, Characterizing the  
727 variability and meteorological drivers of wind power and solar power  
728 generation over africa, *Meteorological Applications* 29 (5) (2022) e2093.  
729 doi:<https://doi.org/10.1002/met.2093>.
- 730 [15] P. T. Brown, D. J. Farnham, K. Caldeira, Meteorology and climatology  
731 of historical weekly wind and solar power resource droughts over western  
732 north america in ERA5, *SN Applied Sciences* 3 (10) (sep 2021). doi:  
733 <https://doi.org/10.1007/s42452-021-04794-z>.
- 734 [16] K. Doering, S. Steinschneider, Summer covariability of surface climate  
735 for renewable energy across the contiguous united states: Role of the  
736 north atlantic subtropical high, *Journal of Applied Meteorology and Cli-*  
737 *matology* 57 (12) (2018) 2749–2768. doi:<https://doi.org/10.1175/jamc-d-18-0088.1>.
- 739 [17] K. Z. Rinaldi, J. A. Dowling, T. H. Ruggles, K. Caldeira, N. S. Lewis,  
740 Wind and solar resource droughts in california highlight the bene-  
741 fits of long-term storage and integration with the western intercon-  
742 nect, *Environmental Science & Technology* 55 (9) (2021) 6214–6226.  
743 doi:<https://doi.org/10.1021/acs.est.0c07848>.
- 744 [18] Y. Amonkar, D. J. Farnham, U. Lall, A k-nearest neighbor space-time  
745 simulator with applications to large-scale wind and solar power model-  
746 ing, *Patterns* 3 (3) (2022) 100454. doi:<https://doi.org/10.1016/j.patter.2022.100454>.
- 748 [19] D. Zheng, D. Tong, S. J. Davis, Y. Qin, Y. Liu, R. Xu, J. Yang, X. Yan,  
749 G. Geng, H. Che, Q. Zhang, Climate change impacts on the extreme  
750 power shortage events of wind-solar supply systems worldwide during  
751 1980–2022, *Nature Communications* 15 (1) (Jun. 2024). doi:<https://doi.org/10.1038/s41467-024-48966-y>.
- 753 [20] M. Ghosal, A. M. Campbell, M. A. Elizondo, N. A. Samaan, Q. H.  
754 Nguyen, T. B. Nguyen, C. Muñoz, D. M. Hernández, Grid reserve and  
755 flexibility planning tool (graf-plan) for assessing resource balancing ca-  
756 pability under high renewable penetration, *IEEE Open Access Journal*  
757 *of Power and Energy* 10 (2023) 560–571. doi:<https://doi.org/10.1109/OAJPE.2022.3169729>.
- 758

- 759 [21] O. J. Guerra, J. Zhang, J. Eichman, P. Denholm, J. Kurtz, B.-M. Hodge,  
760 The value of seasonal energy storage technologies for the integration of  
761 wind and solar power, *Energy & Environmental Science* 13 (7) (2020)  
762 1909–1922. doi:<https://doi.org/10.1039/D0EE00771D>.
- 763 [22] A. Zeighami, J. Kern, A. J. Yates, P. Weber, A. A. Bruno, U.s. west  
764 coast droughts and heat waves exacerbate pollution inequality and can  
765 evade emission control policies, *Nature Communications* 14 (1) (Mar.  
766 2023). doi:<https://doi.org/10.1038/s41467-023-37080-0>.
- 767 [23] N. Voisin, M. Kintner-Meyer, D. Wu, R. Skaggs, T. Fu, T. Zhou,  
768 T. Nguyen, I. Kraucunas, Opportunities for joint water–energy man-  
769 agement: Sensitivity of the 2010 western u.s. electricity grid oper-  
770 ations to climate oscillations, *Bulletin of the American Meteorologi-  
771 cal Society* 99 (2) (2018) 299–312. doi:[https://doi.org/10.1175/  
772 bams-d-16-0253.1](https://doi.org/10.1175/bams-d-16-0253.1).
- 773 [24] F. A. Wolak, Long-term resource adequacy in wholesale electricity mar-  
774 kets with significant intermittent renewables, *Environmental and Energy  
775 Policy and the Economy* 3 (2022) 155–220. doi:[https://doi.org/10.  
776 1086/717221](https://doi.org/10.1086/717221).
- 777 [25] R. Schroeder, A. Joyeau, E. M. Carlini, Seasonal adequacy risks, in:  
778 2018 IEEE International Conference on Environment and Electrical  
779 Engineering and 2018 IEEE Industrial and Commercial Power Sys-  
780 tems Europe (EEEIC / I&CPS Europe), IEEE, 2018, pp. 1–6. doi:  
781 10.1109/eeeic.2018.8494396.
- 782 [26] B. François, H. Puspitarini, E. Volpi, M. Borga, Statistical analysis of  
783 electricity supply deficits from renewable energy sources across an alpine  
784 transect, *Renewable Energy* 201 (2022) 1200–1212. doi:[https://doi.  
785 org/10.1016/j.renene.2022.10.125](https://doi.org/10.1016/j.renene.2022.10.125).
- 786 [27] L. v. d. Most, K. v. d. Wiel, W. Gerbens-Leenes, R. R. Benders, R. Bin-  
787 tanja, Temporally compounding energy droughts in european electric-  
788 ity systems with hydropower, *Nature Energy* (Jan. 2024). doi:<https://doi.org/10.21203/rs.3.rs-3796061/v1>.
- 790 [28] A. Wörman, I. Pechlivanidis, D. Mewes, J. Riml, C. Bertacchi Uvo,  
791 Spatiotemporal management of solar, wind and hydropower across con-

- 792 tinentaleurope, *Communications Engineering* 3 (1) (Jan. 2024). doi:  
793 <https://doi.org/10.1038/s44172-023-00155-3>.
- 794 [29] A. Somani, S. Datta, S. Kincic, V. Chalishazar, B. Vyakaranam,  
795 N. Samaan, A. Colotelo, Y. Zhang, V. Koritarov, T. McJunkin,  
796 T. Mosier, J. Novacheck, M. Emmanuel, M. Schwarz, L. Markel,  
797 C. O'Reilley, *Hydropower's contributions to grid resilience*, Tech. rep.,  
798 Pacific Northwest National Laboratory (2021).
- 799 [30] D. Tong, D. J. Farnham, L. Duan, Q. Zhang, N. S. Lewis, K. Caldeira,  
800 S. J. Davis, *Geophysical constraints on the reliability of solar and wind  
801 power worldwide*, *Nature Communications* 12 (1) (2021) 6146. doi:  
802 <https://doi.org/10.1038/s41467-021-26355-z>.
- 803 [31] K. Engeland, M. Borga, J.-D. Creutin, B. François, M.-H. Ramos, J.-  
804 P. Vidal, *Space-time variability of climate variables and intermittent  
805 renewable electricity production – a review*, *Renewable and Sustainable  
806 Energy Reviews* 79 (2017) 600–617. doi:[https://doi.org/10.1016/  
807 j.rser.2017.05.046](https://doi.org/10.1016/j.rser.2017.05.046).
- 808 [32] K. Mohammadi, N. Goudarzi, *Study of inter-correlations of solar radia-  
809 tion, wind speed and precipitation under the influence of el niño southern  
810 oscillation (enso) in california*, *Renewable Energy* 120 (2018) 190–200.  
811 doi:<https://doi.org/10.1016/j.renene.2017.12.069>.
- 812 [33] L. Lledó, O. Bellprat, F. J. Doblas-Reyes, A. Soret, *Investigating the  
813 effects of pacific sea surface temperatures on the wind drought of  
814 2015 over the united states*, *Journal of Geophysical Research: Atmo-  
815 spheres* 123 (10) (2018) 4837–4849. doi:[https://doi.org/10.1029/  
816 2017JD028019](https://doi.org/10.1029/2017JD028019).
- 817 [34] K. van der Wiel, L. Stoop, B. van Zuijlen, R. Blackport, M. van den  
818 Broek, F. Selten, *Meteorological conditions leading to extreme low  
819 variable renewable energy production and extreme high energy short-  
820 fall*, *Renewable and Sustainable Energy Reviews* 111 (2019) 261–275.  
821 doi:<https://doi.org/10.1016/j.rser.2019.04.065>.
- 822 [35] H. C. Bloomfield, D. J. Brayshaw, A. J. Charlton-Perez, *Characterizing  
823 the winter meteorological drivers of the european electricity system using*

- 824 targeted circulation types, *Meteorological Applications* 27 (1) (2020)  
825 e1858. doi:<https://doi.org/10.1002/met.1858>.
- 826 [36] H. C. Bloomfield, C. C. Suitters, D. R. Drew, Meteorological drivers of  
827 european power system stress, *Journal of Renewable Energy* 2020 (2020)  
828 5481010. doi:<https://doi.org/10.1155/2020/5481010>.
- 829 [37] Y. Liu, S. Feng, Y. Qian, H. Huang, L. K. Berg, How do north ameri-  
830 can weather regimes drive wind energy at the sub-seasonal to seasonal  
831 timescales?, *npj Climate and Atmospheric Science* 6 (1) (Jul. 2023).  
832 doi:<https://doi.org/10.1038/s41612-023-00403-5>.
- 833 [38] D. Rife, N. Y. Krakauer, D. S. Cohan, J. C. Collier, A new kind of  
834 drought: Us record low windiness in 2015, *Earthzine* (2016).  
835 URL <https://earthzine.org/a-new-kind-of-drought-u-s-record-low-windiness-in-2015/>
- 836 [39] X. Yang, T. L. Delworth, L. Jia, N. C. Johnson, F. Lu, C. McHugh,  
837 Skillful seasonal prediction of wind energy resources in the contiguous  
838 united states, *Communications Earth & Environment* 5 (1) (Jun. 2024).  
839 doi:<https://doi.org/10.1038/s43247-024-01457-w>.
- 840 [40] M. Kittel, W.-P. Schill, Measuring the dunkelflaute: How (not) to  
841 analyze variable renewable energy shortage, *Environmental Research:*  
842 *Energy* (Aug. 2024). doi:[https://doi.org/10.1088/2753-3751/](https://doi.org/10.1088/2753-3751/ad6dfc)  
843 [ad6dfc](https://doi.org/10.1088/2753-3751/ad6dfc).
- 844 [41] C. Bracken, Y. Son, D. Broman, N. Voisin, Godeeep-hydro: Historical  
845 and projected power system ready hydropower data for the united states,  
846 *Scientific Data* (2024).
- 847 [42] A. D. Jones, D. Rastogi, P. Vahmani, A. M. Stansfield, K. A. Reed,  
848 T. Thurber, P. A. Ullrich, J. S. Rice, Continental united states cli-  
849 mate projections based on thermodynamic modification of historical  
850 weather, *Scientific Data* 10 (1) (sep 2023). doi:[https://doi.org/10.](https://doi.org/10.1038/s41597-023-02485-5)  
851 [1038/s41597-023-02485-5](https://doi.org/10.1038/s41597-023-02485-5).
- 852 [43] W. C. Skamarock, J. B. Klemp, J. Dudhia, D. O. Gill, Z. Liu, J. Berner,  
853 W. Wang, J. G. Powers, M. G. Duda, D. M. Barker, X.-Y. Huang, A de-  
854 scription of the advanced research wrf model version 4, Report, National  
855 Center for Atmospheric Research (2019). doi:10.5065/1dfh-6p97.  
856 URL <http://dx.doi.org/10.5065/1dfh-6p97>

- 857 [44] H. Hersbach, B. Bell, P. Berrisford, S. Hirahara, A. Horányi, J. Muñoz-  
858 Sabater, J. Nicolas, C. Peubey, R. Radu, D. Schepers, A. Simmons,  
859 C. Soci, S. Abdalla, X. Abellan, G. Balsamo, P. Bechtold, G. Bia-  
860 vati, J. Bidlot, M. Bonavita, G. Chiara, P. Dahlgren, D. Dee, M. Dia-  
861 mantakis, R. Dragani, J. Flemming, R. Forbes, M. Fuentes, A. Geer,  
862 L. Haimberger, S. Healy, R. J. Hogan, E. Hólm, M. Janisková, S. Kee-  
863 ley, P. Laloyaux, P. Lopez, C. Lupu, G. Radnoti, P. Rosnay, I. Rozum,  
864 F. Vamborg, S. Villaume, J.-N. Thépaut, The ERA5 global reanalysis,  
865 *Quarterly Journal of the Royal Meteorological Society* 146 (730) (2020)  
866 1999–2049. doi:<https://doi.org/10.1002/qj.3803>.
- 867 [45] EIA, Form EIA-860 detailed data with previous form data (EIA-  
868 860A/860B), <https://www.eia.gov/electricity/data/eia860/>  
869 (Sep. 2022).
- 870 [46] G. Buster, M. Rossol, P. Pinchuk, R. Spencer, B. N. Benton, M. Ban-  
871 nister, T. Williams, The renewable energy potential model (rev) (Feb.  
872 2023). doi:<https://doi.org/10.5281/zenodo.7641483>.
- 873 [47] M. Sengupta, Y. Xie, A. Lopez, A. Habte, G. Maclaurin, J. Shelby, The  
874 national solar radiation data base (NSRDB), *Renewable and Sustainable*  
875 *Energy Reviews* 89 (2018) 51–60. doi:[https://doi.org/10.1016/j.](https://doi.org/10.1016/j.rser.2018.03.003)  
876 [rser.2018.03.003](https://doi.org/10.1016/j.rser.2018.03.003).
- 877 [48] A. Campbell, C. Bracken, S. Underwood, N. Voisin, A multi-decadal  
878 hourly coincident wind and solar power production dataset for the con-  
879 tiguous us, Submitted (2024).
- 880 [49] X. Liang, D. P. Lettenmaier, E. F. Wood, S. J. Burges, A simple hydro-  
881 logically based model of land surface water and energy fluxes for gen-  
882 eral circulation models, *Journal of Geophysical Research: Atmospheres*  
883 99 (D7) (2012) 14415–14428. doi:[10.1029/94jd00483](https://doi.org/10.1029/94jd00483).  
884 URL [https://agupubs.onlinelibrary.wiley.com/doi/pdfdirect/](https://agupubs.onlinelibrary.wiley.com/doi/pdfdirect/10.1029/94JD00483?download=true)  
885 [10.1029/94JD00483?download=true](https://agupubs.onlinelibrary.wiley.com/doi/pdfdirect/10.1029/94JD00483?download=true)
- 886 [50] J. J. Hamman, B. Nijssen, T. J. Bohn, D. R. Gergel, Y. Mao,  
887 The variable infiltration capacity model version 5 (vic-5): in-  
888 frastructure improvements for new applications and reproducibil-  
889 ity, *Geoscientific Model Development* 11 (8) (2018) 3481–3496.  
890 doi:[10.5194/gmd-11-3481-2018](https://doi.org/10.5194/gmd-11-3481-2018).

- 891 URL [https://gmd.copernicus.org/articles/11/3481/2018/](https://gmd.copernicus.org/articles/11/3481/2018/gmd-11-3481-2018.pdf)  
892 [gmd-11-3481-2018.pdf](https://gmd.copernicus.org/articles/11/3481/2018/gmd-11-3481-2018.pdf)
- 893 [51] Y. Yang, M. Pan, H. E. Beck, C. K. Fisher, R. E. Beighley, S.-C. Kao,  
894 Y. Hong, E. F. Wood, In quest of calibration density and consistency in  
895 hydrologic modeling: Distributed parameter calibration against stream-  
896 flow characteristics, *Water Resources Research* 55 (9) (2019) 7784–7803.  
897 doi:<https://doi.org/10.1029/2018WR024178>.
- 898 [52] Y. Yang, M. Pan, P. R. Lin, H. E. Beck, Z. Z. Zeng, D. Yamazaki,  
899 C. H. David, H. Lu, K. Yang, Y. Hong, E. F. Wood, Global reach-level  
900 3-hourly river flood reanalysis (1980-2019), *Bulletin of the American Me-*  
901 *teorological Society* 102 (11) (2021) E2086–E2105, zc1gv Times Cited:25  
902 Cited References Count:100. doi:[10.1175/Bams-D-20-0057.1](https://doi.org/10.1175/Bams-D-20-0057.1).  
903 URL <GotoISI>:[//WOS:000757278200004](https://wos.000757278200004)
- 904 [53] T. Thurber, C. Vernon, N. Sun, S. Turner, J. Yoon, N. Voisin,  
905 mosartwmpy: A python implementation of the mosart-wm coupled hy-  
906 drologic routing and water management model, *Journal of Open Source*  
907 *Software* 6 (62) (2021). doi:[10.21105/joss.03221](https://doi.org/10.21105/joss.03221).  
908 URL <https://joss.theoj.org/papers/10.21105/joss.03221.pdf>
- 909 [54] H. Y. Li, M. S. Wigmosta, H. Wu, M. Y. Huang, Y. H. Ke, A. M.  
910 Coleman, L. R. Leung, A physically based runoff routing model for land  
911 surface and earth system models, *Journal of Hydrometeorology* 14 (3)  
912 (2013) 808–828, 162xz Times Cited:158 Cited References Count:61. doi:  
913 [10.1175/Jhm-D-12-015.1](https://doi.org/10.1175/Jhm-D-12-015.1).
- 914 [55] N. Voisin, H. Li, D. Ward, M. Huang, M. Wigmosta, L. R. Leung, On  
915 an improved sub-regional water resources management representation  
916 for integration into earth system models, *Hydrology and Earth System*  
917 *Sciences* 17 (9) (2013) 3605–3622. doi:[10.5194/hess-17-3605-2013](https://doi.org/10.5194/hess-17-3605-2013).  
918 URL [https://hess.copernicus.org/articles/17/3605/2013/](https://hess.copernicus.org/articles/17/3605/2013/hess-17-3605-2013.pdf)  
919 [hess-17-3605-2013.pdf](https://hess.copernicus.org/articles/17/3605/2013/hess-17-3605-2013.pdf)
- 920 [56] S. W. D. Turner, J. C. Steyaert, L. Condon, N. Voisin, Water stor-  
921 age and release policies for all large reservoirs of conterminous united  
922 states, *Journal of Hydrology* 603 (2021). doi:[10.1016/j.jhydrol.](https://doi.org/10.1016/j.jhydrol.2021.126843)  
923 [2021.126843](https://doi.org/10.1016/j.jhydrol.2021.126843).

- 924 [57] D. Broman, N. Voisin, S.-C. Kao, A. Fernandez, G. R. Ghimire, Multi-  
925 scale impacts of climate change on hydropower for long-term water-  
926 energy planning in the contiguous united states, *Environmental Re-*  
927 *search Letters* 19 (9) (2024) 094057. doi:[https://doi.org/10.1088/](https://doi.org/10.1088/1748-9326/ad6ceb)  
928 [1748-9326/ad6ceb](https://doi.org/10.1088/1748-9326/ad6ceb).
- 929 [58] S. W. D. Turner, N. Voisin, J. Fazio, D. Hua, M. Jourabchi,  
930 Compound climate events transform electrical power shortfall  
931 risk in the pacific northwest, *Nat Commun* 10 (1) (2019) 8.  
932 doi:[10.1038/s41467-018-07894-4](https://doi.org/10.1038/s41467-018-07894-4).  
933 URL <https://www.ncbi.nlm.nih.gov/pubmed/30602781>[https://www.ncbi.nlm.nih.gov/pmc/articles/PMC6315041/pdf/41467\\_](https://www.ncbi.nlm.nih.gov/pmc/articles/PMC6315041/pdf/41467_2018_Article_7894.pdf)  
934 [2018\\_Article\\_7894.pdf](https://www.ncbi.nlm.nih.gov/pmc/articles/PMC6315041/pdf/41467_2018_Article_7894.pdf)  
935
- 936 [59] K. Doering, C. L. Anderson, S. Steinschneider, Evaluating the inten-  
937 sity, duration and frequency of flexible energy resources needed in a  
938 zero-emission, hydropower reliant power system, *Oxford Open Energy*  
939 *2* (2023). doi:<https://doi.org/10.1093/ooenergy/oiad003>.
- 940 [60] Grid Deployment Office, The nationaltransmission planning study,  
941 Tech. rep., U.S. Department of Energy, Grid Deployment Office.  
942 2024. The NationalTransmission Planning Study. Washington, D.C.:  
943 U.S. Department of Energy.[https://www.energy.gov/gdo/national-](https://www.energy.gov/gdo/national-transmission-planning-study)  
944 [transmission-planning-study.](https://www.energy.gov/gdo/national-transmission-planning-study), Washington, D.C. (2024).  
945 URL <https://www.energy.gov/gdo/national-transmission-planning-study>
- 946 [61] F. Mockert, C. M. Grams, T. Brown, F. Neumann, Meteorological condi-  
947 tions during periods of low wind speed and insolation in germany: The  
948 role of weather regimes, *Meteorological Applications* 30 (4) (Jul. 2023).  
949 doi:<https://doi.org/10.1002/met.2141>.
- 950 [62] H. Hersbach, B. Bell, P. Berrisford, G. Biavati, A. Horányi,  
951 J. Muñoz Sabater, J. Nicolas, C. Peubey, R. Radu, I. Rozum, D. Schep-  
952 ers, A. Simmons, C. Soci, D. Dee, J.-N. Thépaut, Era5 hourly data on  
953 single levels from 1940 to present, Copernicus Climate Change Service  
954 (C3S) Climate Data Store (CDS) (2023). doi:[https://doi.org/10.](https://doi.org/10.24381/cds.adbb2d47)  
955 [24381/cds.adbb2d47](https://doi.org/10.24381/cds.adbb2d47).
- 956 [63] J. Larson, Y. Zhou, R. W. Higgins, Characteristics of landfalling tropical  
957 cyclones in the united states and mexico: *Climatology and interannual*

- 958 variability, *Journal of Climate* 18 (8) (2005) 1247–1262. doi:<https://doi.org/10.1175/JCLI3317.1>.  
959
- 960 [64] R. W. Higgins, A. Leetmaa, Y. Xue, A. Barnston, Dominant  
961 factors influencing the seasonal predictability of u.s. precipitation  
962 and surface air temperature, *Journal of Climate* 13 (22) (2000)  
963 3994–4017. doi:[https://doi.org/10.1175/1520-0442\(2000\)013%3C3994:DFITSP%3E2.0.CO%3B2](https://doi.org/10.1175/1520-0442(2000)013%3C3994:DFITSP%3E2.0.CO%3B2).  
964
- 965 [65] R. W. Higgins, A. Leetmaa, V. E. Kousky, Relationships between cli-  
966 mate variability and winter temperature extremes in the united states,  
967 *Journal of Climate* 15 (13) (2002) 1555–1572. doi:[https://doi.org/10.1175/1520-0442\(2002\)015%3C1555:RBCVAW%3E2.0.CO%3B2](https://doi.org/10.1175/1520-0442(2002)015%3C1555:RBCVAW%3E2.0.CO%3B2).  
968
- 969 [66] A. G. Barnston, R. E. Livezey, Classification, seasonality and persistence  
970 of low-frequency atmospheric circulation patterns, *Monthly Weather*  
971 *Review* 115 (6) (1987) 1083–1126. doi:[https://doi.org/10.1175/1520-0493\(1987\)115%3C1083:CSAPOL%3E2.0.CO%3B2](https://doi.org/10.1175/1520-0493(1987)115%3C1083:CSAPOL%3E2.0.CO%3B2).  
972
- 973 [67] S. Curtis, R. Adler, Enso indices based on patterns of satellite-  
974 derived precipitation, *Journal of Climate* 13 (15) (2000) 2786–2793.  
975 doi:[https://doi.org/10.1175/1520-0442\(2000\)013%3C2786:  
976 EIBOPO%3E2.0.CO%3B2](https://doi.org/10.1175/1520-0442(2000)013%3C2786:EIBOPO%3E2.0.CO%3B2).
- 977 [68] Western Electricity Coordinating Council (WECC), 2030 ADS PCM  
978 release notes, [https://www.wecc.org/Reliability/2030ADS\\_PCM\\_  
979 ReleaseNotes\\_GV-V2.3\\_6-9-2021.pdf](https://www.wecc.org/Reliability/2030ADS_PCM_ReleaseNotes_GV-V2.3_6-9-2021.pdf) (2024).
- 980 [69] O. Anderson, C. Bracken, C. D. Burleyson, A. Pusch, N. Yu, Improved  
981 decarbonization planning through climate resiliency modeling, *IEEE Ac-  
982 cess* 12 (2024) 128494–128508. doi:[10.1109/access.2024.3451957](https://doi.org/10.1109/access.2024.3451957).
- 983 [70] Y. Ou, G. Iyer, H. McJeon, R. Cui, A. Zhao, K. T. O’Keefe, M. Zhao,  
984 Y. Qiu, D. H. Loughlin, State-by-state energy-water-land-health impacts  
985 of the us net-zero emissions goal, *Energy and Climate Change* 4 (2023)  
986 100117. doi:<https://doi.org/10.1016/j.egycc.2023.100117>.
- 987 [71] Y. Ou, Y. Zhang, S. Waldhoff, G. Iyer, Gcam-usa scenarios for godeeep  
988 (2024). doi:<https://doi.org/10.5281/ZENODO.10642507>.

989 [72] D. Yates, J. K. Szinai, A. D. Jones, Modeling the water systems of  
990 the western us to support climate-resilient electricity system planning,  
991 Earth's Future 12 (1) (Dec. 2023). doi:[https://doi.org/10.1029/  
992 2022EF003220](https://doi.org/10.1029/2022EF003220).